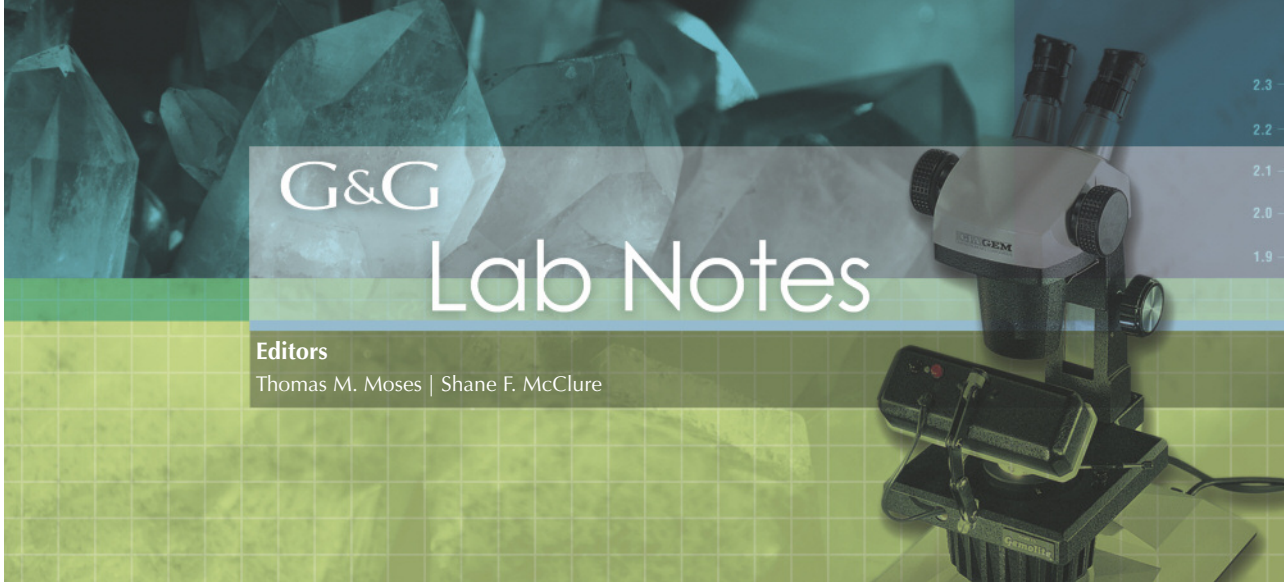

Unusual Graining Structure in Pink DIAMOND

Natural pink diamonds examined for origin of color determination often display visible pink coloring along planes of stress. This graining is visible at a slight angle to the plane and can occur as a single plane or multiple parallel planes. The color may be either uniform or unevenly distributed along the graining. One pink stone recently examined in the Carlsbad lab was noted to have a uniform plane of pink color with a colorless hole (figure 1, left). The diamond was graded Very Light pink, so the colored plane had low saturation, but the irregularity was impossible to miss in the microscope. When examined under polarized light, a cone of strain could be seen intersecting the plane and fitting perfectly in the colorless hole (figure 1, right).

Pink graining is the result of an unknown defect with an unknown formation mechanism (J.G. Chapman and C.J. Noble, "Studies of the pink and blue coloration in Argyle diamonds," Summer 1999 *G&G*, pp. 156–157). It seems to be related to the plastic deformation of diamond, evidenced by the color lying along planes of stress. Whether pink graining occurs during diamond growth or is formed after by stresses or heat from the earth (or a combination of the two) is also poorly understood. It is therefore a mystery as to whether the cone of strain formed first or concurrently and prevented the formation of pink graining at the circle of intersection, or if the cone formed afterward and destroyed the color centers associated with pink graining. Until diamond formation is more fully understood, this dynamic interplay of strain will remain a mystery.

Troy Ardon

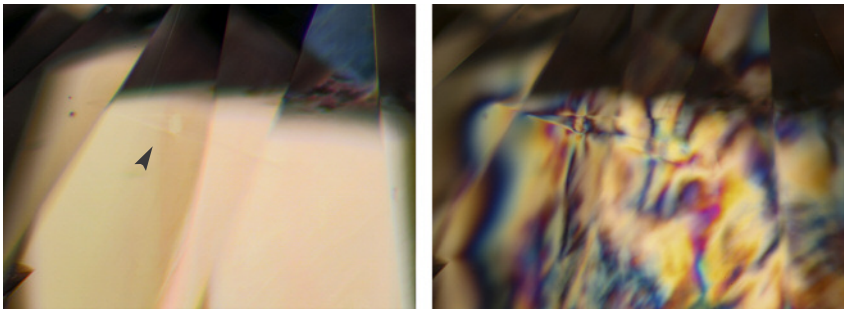

Figure 1. Left: A colorless hole within a natural pink diamond, observed with darkfield illumination. Field of view approximately 2 mm. Right: The colorless hole in polarized light, showing the cone of strain. Field of view approximately 2 mm.

Editors' note: All items were written by staff members of GIA laboratories.

Gems & Gemology, Vol. 51, No. 3, pp. 312–322.

Yellow HPHT-Processed Rough Diamond

High-pressure, high-temperature (HPHT) annealing is a very effective method for changing the color of diamonds, particularly those with an undesirable brownish color. This treatment process has been practiced in the trade for more than 15 years. An important feature of this treatment is the etching often left behind on the diamond surfaces. Recently, one loose yellow diamond rough, weighing 2.47 ct and measuring 7.09 × 6.59 × 5.46 mm, was examined in the New York lab (figure 2). Without magnification, the rough had a vibrant yellow color and an overall clean-looking surface. Closer microscopic observation showed a very slightly etched surface, as well as some altered graphitized crystal inclusions in the diamond. Distinctive fluorescence reactions to long- and short-wave ultraviolet radiation similar to those of HPHT-processed material were observed, with a medium chalky bluish green under long-wave and medium to strong

Figure 2. This 2.47 ct rough diamond was HPHT processed to improve its color. Unlike conventional HPHT-treated diamonds, this stone has a natural-looking surface.

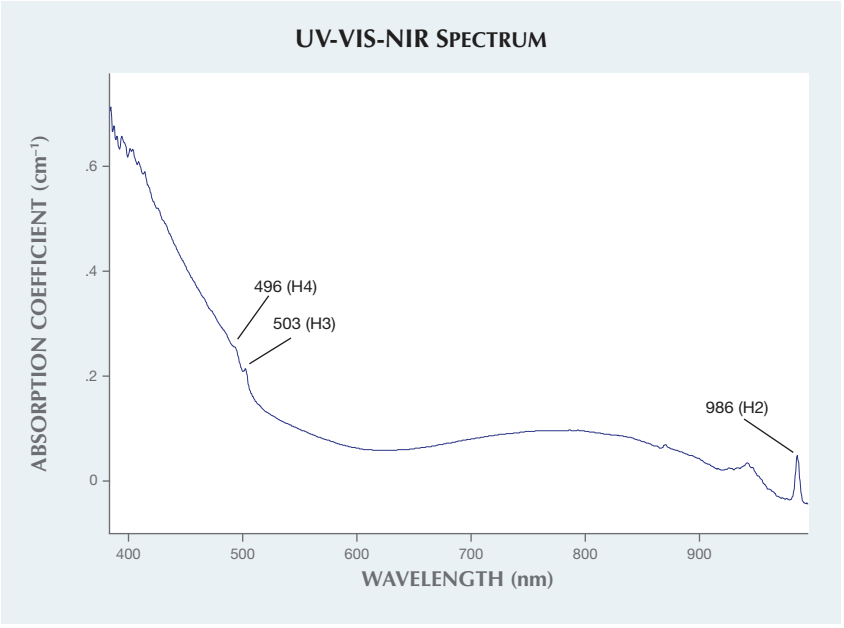

Figure 3. The yellow rough's UV-Vis-NIR spectrum, showing H2 (986 nm), H3 (503 nm), and H4 (496 nm) peaks, indicates HPHT treatment.

greenish yellow under short-wave UV. This was suspect, and further testing was needed. UV-Vis-NIR and mid-IR spectroscopy revealed the rough diamond to be HPHT processed.

The UV-Vis-NIR spectrum, seen in figure 3, showed a rise in absorption from 500 nm, associated with strong H3 (503 nm) and H4 (496 nm) peaks, along with a sharp H2 (986 nm) peak. These are indicative of HPHT treatment. Mid-IR spectroscopy (figure 4) revealed peaks at 1170 and 1332 cm^{-1}, indicating that the starting material of this diamond appeared to be type IaB. The high temperature and high pressure of the treatment created isolated nitrogen with a corresponding absorption peak detected at 1344 cm^{-1}. Occurrence of isolated nitrogen in a pure type IaB diamond is a strong indicator of HPHT treatment.

The majority of HPHT-treated rough diamonds have severely burned, etched, and pitted surfaces. This is the first time we have seen an almost eye-clean yellow rough post-HPHT treatment. With new technologies available to diamond merchants, HPHT processing techniques are becoming more sophisticated, allowing for the retention of carat weight during the cutting process. This case serves as a clear reminder that buying rough does not assure a lack of treatment.

Sally Chan

Figure 4. Mid-IR spectroscopy revealed an absorption peak at 1344 cm^{-1}, indicating the presence of isolated nitrogen. This occurrence and corresponding peak are characteristic of HPHT processing.

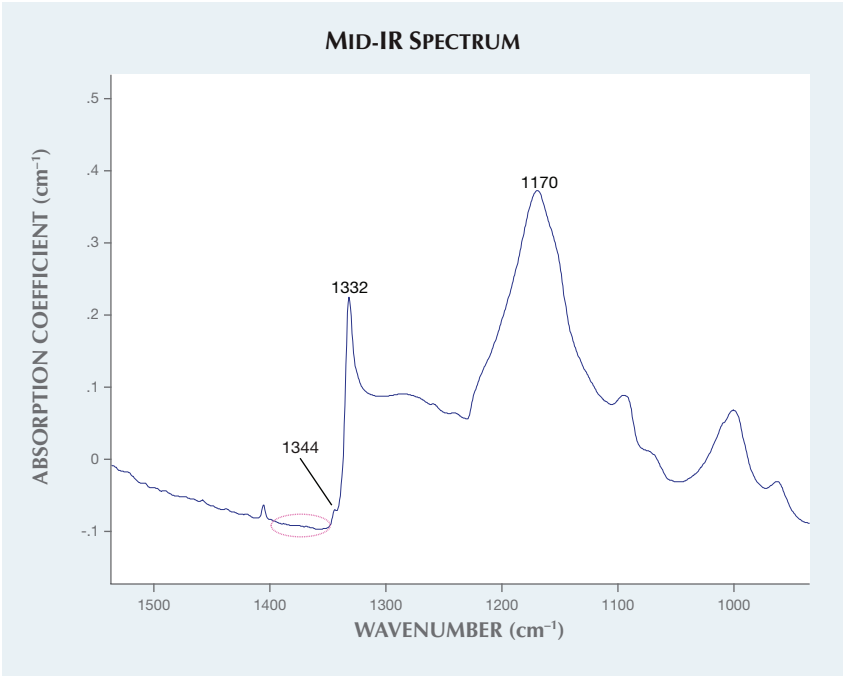

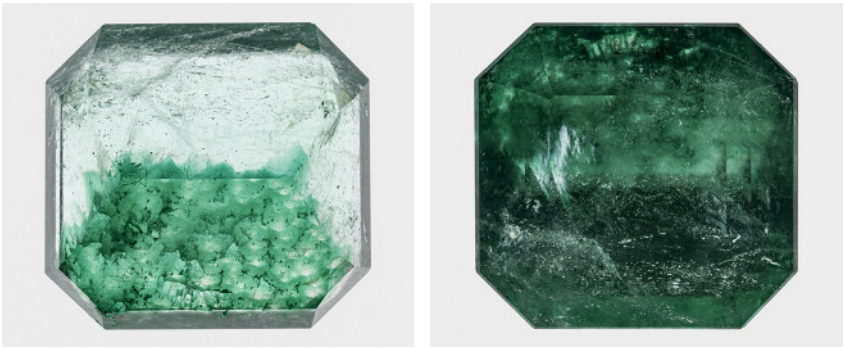

Figure 5. Left: When table-down, the stone is mainly colorless, showing some partially green overgrowth. Right: Face-up, the faceted stone displays an even and attractive dark green emerald color.

Color-Zoned EMERALD

Cutting style and orientation are important considerations when cutting natural crystals with strong color zoning. Careful placement of these zones can distribute color by reflection, creating a uniformly colored finished stone when viewed face-up.

Recently, the Carlsbad laboratory received a 33.73 ct green octagonal step cut showing strong color zoning (figure 5). The gem cutter skillfully placed a thin green color zone in this emerald along the pavilion facets so that the stone would appear uniformly green when in a face-up position. Standard gemological testing revealed a refractive index (RI) of 1.571–1.578 and a specific gravity (SG) of 2.72. Chromium-related features were observed in the red end of the spectrum when examined with a handheld spectroscope. All of these properties were consistent with emerald. During microscopic examination, minute jagged fluid inclusions and growth tubes were observed, proving the stone was of natural origin (figure 6).

Interestingly, the stone showed a strong green color zone very close to some of the pavilion facets, as well as hexagonal columnar-like growth and irregular zoning (figure 7). This type of zoning represents a late-stage influx of chromium and vanadium into the genetic environment, which were then incorporated into the crystal lattice of the beryl. EDXRF revealed high levels of Cr and V in the green color zone, which was consistent with the observed color. Although similar zoning has been observed in emerald previously (E.J. Gübelin and J.I. Koivula, *Photoatlas of Inclusions in Gemstones, Volume 3*, Opinio Verlag, Basel, Switzerland, 2008, pp. 433–434), the zoning in this specimen was quite distinct.

This emerald demonstrates the significance of proper orientation and cutting style in fashioning high-quality gem materials.

Jonathan Muyal, Nathan Renfro, and Amy Cooper

Figure 6. When viewed from the side, irregular green color zoning is observed along with minute jagged fluid inclusions. Field of view 14.52 mm.

Figure 7. The colorless spots indicate parallel columnar growth of white beryl overgrown by green emerald. Field of view 19.27 mm.

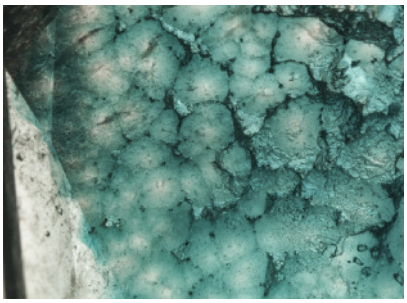

Orange Faceted EOSPHORITE

The Carlsbad laboratory recently examined a 5.85 ct transparent orange oval mixed cut for identification services (figure 8). Standard gemological testing showed an RI of 1.640 to 1.667; the hydrostatic SG was 3.12. The stone showed yellow and reddish orange pleochroism. Fluorescence was inert to long-wave and short-wave UV radiation. The most distinctive internal characteristic, revealed by microscopic examination, was the presence of multiphase inclusions (figure 9), suggesting a formation process with the presence of water, such as pegmatitic and hydrothermal processes.

Figure 8. This 5.85 ct orange mixed cut was a rare faceted eosphorite.

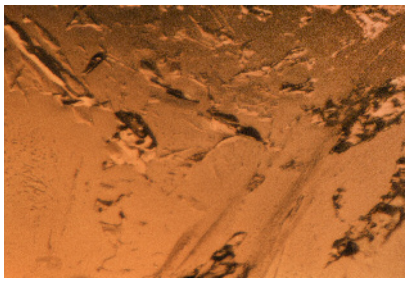

Figure 9. Multi-phase primary fluid inclusions are seen in the eosphorite, indicating a pegmatitic or hydrothermal formation process. Field of view 1.26 mm.

Raman spectroscopy confirmed that the stone belongs to the childrenite-eosphorite mineral series (figure 10), with intense peaks observed at 970 and 1011 cm^{-1}. These peaks are attributed to the P-O (phosphorus-oxygen) stretching vibrations (R. L. Frost et al., "Vibrational spectroscopic characterization of the phosphate mineral series eosphorite-childrenite-(Mn,Fe)Al$(PO_4)(OH)_2 \cdot (H_2O)$," *Vibrational Spectroscopy*, 2013, Vol. 67, pp. 14–21). This mineral series has a stoichiometric formula (Mn,Fe)Al$(PO_4)(OH)_2 \cdot (H_2O)$. Visible absorption spectroscopy revealed that the stone's orange color results from the combination of Fe and Mn (M.A. Hoyos et al., "New structural and spectroscopic data for eosphorite," *Mineralogical Magazine*, 1993, Vol. 57, pp. 329–336).

Energy-dispersive X-ray fluorescence (EDXRF) analysis revealed a composition of 25.10 wt.% Al_2O_3, 31.74 wt.% P_2O_5, 15.46 wt.% MnO, 11.47 wt.% FeO_{tot}, 0.49 wt.% MgO, 0.25 wt.% CaO, and 15.50 wt.% H_2O (water weight percent is assumed from references). The stone contains 55.3 mol.% eosphorite and 40.5 mol.% childrenite. The calculated formula is $(Mn_{0.48}Fe_{0.35}Ca_{0.01}Mg_{0.03})(Al)_{1.09}(P_{0.99}O_4)(OH)_2 \cdot 0.91(H_2O)$, which indicates an intermediate member of the childrenite-eosphorite series with predominance of the Mn phase. As a result, the stone should be classified as eosphorite.

Eosphorite is the manganese-rich end member of the childrenite-eosphorite series, formed worldwide in pegmatites (T. J. Campbell and W. L. Roberts, "Phosphate minerals from the Tip Top mine, Black Hills, South Dakota," *Mineralogical Record*, 1986, Vol. 17, pp. 237–254) or by hydrothermal phosphatization of metasediments and associated with the intrusion of granites (R. S. W. Braithwaite and B. V. Cooper, "Childrenite in South-West England," *Mineralogical Magazine*, 1982, Vol. 46, pp. 119–126). This was the first faceted eosphorite examined by GIA's Carlsbad laboratory.

Figure 10. Raman analysis of the eosphorite in the 2000–200 cm^{-1} range showed a typical spectrum of phosphate oxyanions. The 970 and 1011 cm^{-1} peaks are assigned to the P-O stretching vibration, while the 1038 and 1055 cm^{-1} peaks are attributed to the PO_4^{3-} stretching vibration. The 405, 473, 561, 595, and 618 cm^{-1} peaks are associated with the PO_4 and H_2PO_4 bending modes.

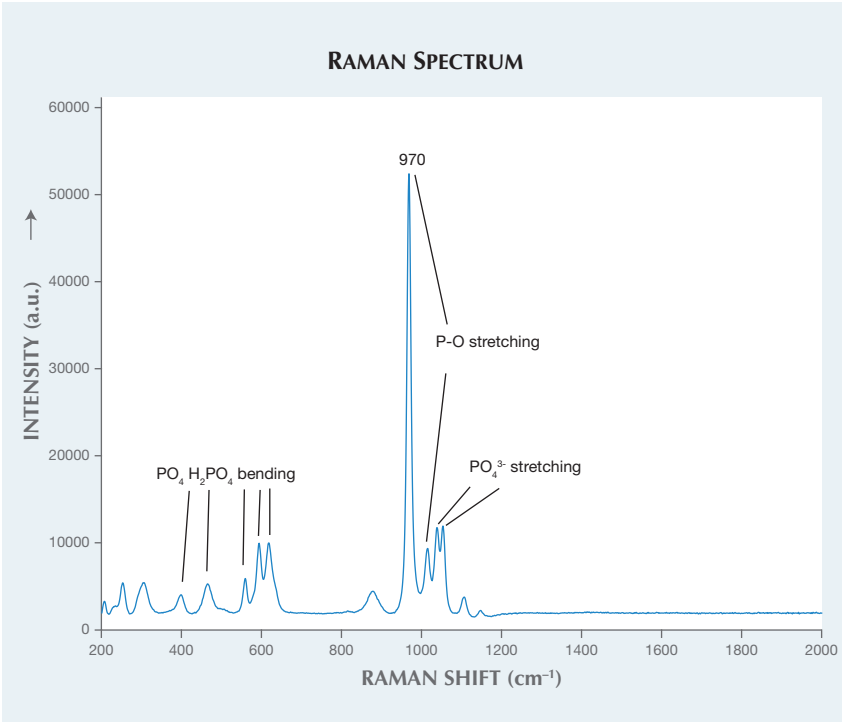

Ziyin Sun, Nathan Renfro, and Amy Cooper

Large Faceted HIBONITE

The Carlsbad laboratory recently examined an unusually large 134.43 ct opaque, very dark brown faceted hibonite (figure 11). Standard gemological testing gave spot RI values of 1.79 to 1.81 and a hydrostatic SG of 3.81. Hibonite, which crystallizes in the hexagonal system, has published RI values of 1.790 to 1.807, but we were unable to observe birefringence, probably due to its opacity and these values' proximity to the limits of the refractometer. The stone showed a high luster and was inert to LW and SWUV. Testing with a Geiger counter showed it was slightly radioactive. All of these features are consistent with hibonite, yet more advanced testing was needed for a positive identification of this unusual material.

Raman spectroscopy gave a spectrum consistent with hibonite. Laser ablation–inductively coupled plasma–mass spectrometry (LA-ICP-MS) analysis revealed large amounts of

Figure 11. This 134.43 ct faceted hibonite is the largest examined by GIA to date.

Mg, Ca, Al, Ti, and Fe; small amounts of Na, Si, Sr, La, and Ce; and traces of numerous other elements, including the radioactive elements thorium (62.62–122.60 ppma) and uranium (0.12–0.56 ppma). The presence of these elements caused the mineral to react to the Geiger counter. The thorium and REE content is consistent with samples from Madagascar (M.A.F. Rakotondrazafy et al., "Mode of formation of hibonite ($CaAl_{12}O_{19}$) within the U-Th skarns from the granulites of S-E Madagascar," *Contributions to Mineralogy and Petrology*, Vol. 123, No. 2, 1996, pp 190–201).

Microscopic examination revealed one deep green mineral inclusion breaking the surface of the table. Its Raman spectrum was consistent with spinel, a known associated mineral of hibonite. LA-ICP-MS analysis showed it was an iron-rich spinel within the hercynite($FeAl_2O_4$)-spinel ($MgAl_2O_4$) series, with almost one-third of the magnesium substituted by iron. Although difficult to see internally, other whitish mineral inclusions were visible, as well as an extensive fracture and cleavage network.

Orangy brown, transparent, and well-formed hexagonal crystals of gem-quality hibonite have been reported from Myanmar (T. Hainschwang et al., "Hibonite: A new gem mineral," Summer 2010 *G&G*, pp. 135–138; Summer 2012 Lab Notes, p. 136). Although not gem quality, the stone's size makes it a rare collector's mineral as well as the largest hibonite GIA has identified to date.

Claire Ito and Ziyin Sun

Dyed and Natural Green JADEITE

The most coveted jadeite stones possess a deep rich green color. Lower-quality jadeite specimens are often treated with acid bleaching, polymer impregnation, and dyes to obtain this sought-after hue (E. Fritsch et al., "Identification of bleached and polymer-impregnated jadeite," Fall 1992 *G&G*, pp. 176–187). It is quite unusual to see stones with even a small amount of natural green color further altered with dyes. When this does happen, the natural properties of the untreated area can make it especially challenging to properly identify the stone as dyed.

Recently, the Carlsbad laboratory examined a carved jadeite specimen (figure 12). Standard gemological testing and Raman spectroscopy confirmed that the specimen was jadeite; infrared spectroscopy indicated the specimen had been polymer impregnated. Observation with a desktop spectroscope revealed lines at 630 and 655 nm, which are associated with chromium impurities in naturally colored green jadeite. Observation under long-wave UV light revealed strong green-yellow fluorescence from most green areas of the stone, but not from the area where Cr lines were seen in the spectroscope. The colorless portions of the stone were also inert to UV light. Strong fluorescence in jadeite is often indicative of either polymer impregnation or a dye treatment; however, fluorescence from polymers would be evenly distributed throughout the stone due to the nature of impregnation. The fact that this stone only fluoresced from the green areas was strong evidence of dyeing rather than impregnation.

Microscopic observation (figure 13) revealed concentrations of green color in the boundary gaps in between grains, typical of dyed jadeite. The green area without fluorescence possessed a smoother, more consistent green color, which is customary for natural jadeite. Absorption spectroscopy in the UV, visible, and near-IR range confirmed that the natural area contained an absorption band from 530 to 740 nm, punctuated by natural chromium peaks at 691 and 655 nm (figure 14). The dyed green areas contained a double band around 627 and 665 nm, which is typical of dyed green jadeite.

The proper treatment identification of jadeite is essential to the consumer's confidence in this stone. Testing only a portion of this material might convince an observer that no

Figure 12. Left: In natural light, the green band in the lower right section of the jadeite specimen is caused by natural chromium, while the other green spots are the result of a dye treatment. Right: Long-wave UV light shows a strong fluorescence from the dyed areas, with little to no fluorescence from the natural green area.

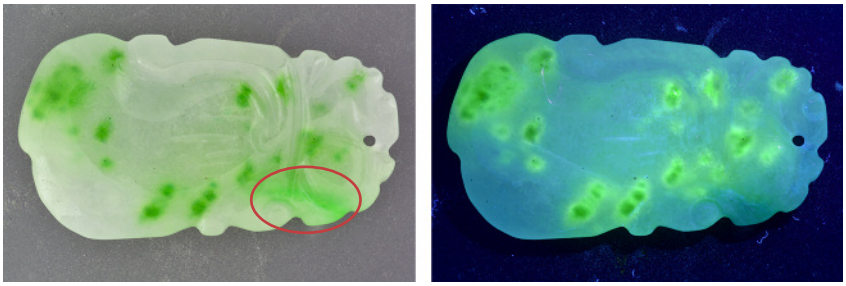

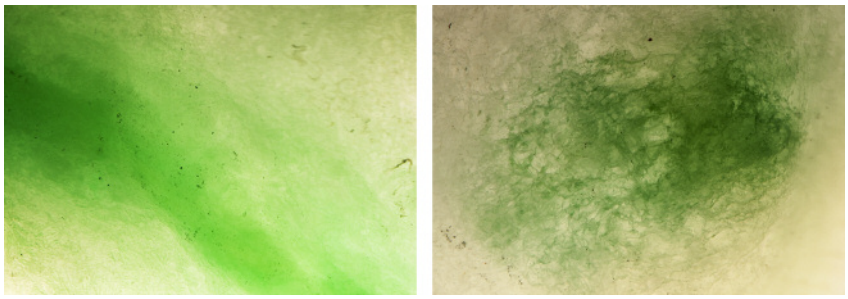

Figure 13. Left: A close-up of the natural green area shows a smooth, diffused color texture. Field of view 7.19 mm. Right: A close-up of a dyed area shows color concentrations in the thin gaps between the crystal grains of jadeite. Field of view 3.57 mm.

dye had been applied. One must always expect the unexpected when attempting to determine treatments in any gemstone.

Dylan Hand

Coated KORNERUPINE Beads

Three dark brown faceted beads with an unusual metallic luster were recently submitted to the Carlsbad laboratory for identification service (figure 15). The three beads ranged from 0.95 ct to 1.38 ct. Standard gemological properties revealed an RI of approximately 1.668–1.680, consistent with kornerupine. The hydrostatic SG ranged from 3.01 to 3.19. This is slightly lower than expected for kornerupine, but can be explained by air trapped in the drill holes. Raman spectroscopy confirmed that the stones were kornerupine.

All three beads exhibited a high metallic luster with silver and bronze coloration, which is not typical for kornerupine. Under microscopic examination with reflected lighting, the surfaces showed spotty luster, consistent with a surface coating (figure 16). Further evidence of coating was visible along the facet junctions, where the coating was worn away.

EDXRF chemical analysis detected large amounts of Mg, Al, and Si, consistent with kornerupine. EDXRF also revealed the presence of copper. The authors could not find documentation

Figure 14. UV-Vis-NIR spectra of the jadeite in the 250–850 nm range showed chromium lines at 655 and 691 nm in the natural green area and double broad bands around 627 and 665 nm in the dyed green area.

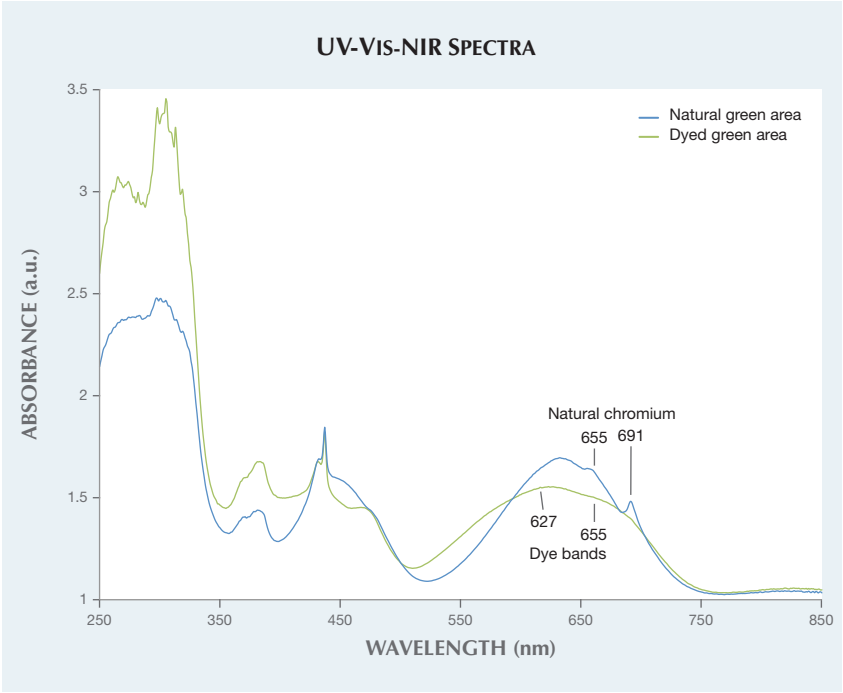

Figure 15. These three kornerupine beads (0.95–1.38 ct) were found to have a metallic coating.

Figure 16. Diffused reflected light exposed spotty luster on the surface of one of the tested stones, indicating the presence of a coating. Field of view 2.17 mm.

of naturally occurring copper in kornerupine, so this element may have been used to create the metallic coating. This is the first time the GIA laboratory has seen coated kornerupine.

Amy Neurauter and Heidi Breitzmann

Assembled Cultured Blister PEARL with an Unusual Component

GIA's Bangkok laboratory recently examined a blue-violet assembled cultured blister pearl (mabe) weighing 2.44 ct and measuring 10.23 × 5.86 mm (figure 17). The specimen had the appearance of a typical mabe pearl, exhibiting a boundary line between the nacre face and shell base. 2D microradiography showed a component with an unusual fluted shape, with radio-translucency similar to that of the $CaCO_3$ nacre and the shell (figure 18).

GIA has examined the characteristics of mabe pearls used in commercial jewelry over the years (see Lab Notes: Summer 1981, pp. 104–105; Summer 1991, pp. 111–112; Fall 1991, p. 177; Summer 1992, pp. 126–127; Fall 1992, pp. 195–196; Fall 1996, p. 210), but none of these notes mentioned this unusual component. In Bangkok, this feature has been seen five times in mabe pearls submitted for testing since 2010; questions about its identity and purpose have been raised since the first observation.

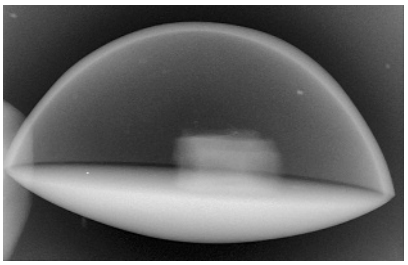

Figure 18. A microradiograph of the intact assembled cultured blister pearl prior to sawing revealed an internal component. The radio-translucency of the object, the nacre, and the shell base are similar.

Out of curiosity, one client decided to cut their sample in half in order to examine the interior in more detail (figure 19, left). The two halves consisted of a thin nacre dome top, which was coated with a dark layer on the inner surface; an artificial resinous material; and the white fluted object bordering the shell base. The fluted object was translucent, and a clear spiderweb structure was visible at 10× magnification. When exposed to standard short-wave UV radiation (254 nm) and examined in the DiamondView, this object showed a moderate white blue reaction that followed the spiderweb pattern (figure 19, right).

Further investigation with Raman spectroscopy using a 488 nm laser revealed a calcite spectrum with peaks at 159, 285, 716, 1088, and 1750 cm^{-1}, similar to white coral (*Corallium secundum*). A small peak related to carotenoid pigments was present at 1020 cm^{-1} (e.g., J. Urmos et al., "Characterization of some biogenic carbonates with Raman spectroscopy," *American Mineralogist*, Vol. 76, 1991, pp. 641–646).

Based on the spiderweb structure, radio-translucency, calcite spectrum, and general appearance, the object appeared to be a biogenic carbonate. White coral was the first material considered. Further research revealed accounts of sea urchin sections used in some assembled cultured blister pearls from Bali, Indonesia, in "Kuta" pearls (E. Strack, *Pearls*, Ruhle-Diebener-Verlag, Stuttgart, Germany, 2006, p. 605). Regardless of identity, the reason for including this material within some mabe pearls remains uncertain. It does not appear related to either the formation of the mabe pearl component or its weight and stability.

Artitaya Homkrajae

Figure 17. This blue-violet assembled cultured blister pearl (mabe) weighed 2.44 carats and measured 10.23 × 5.86 mm.

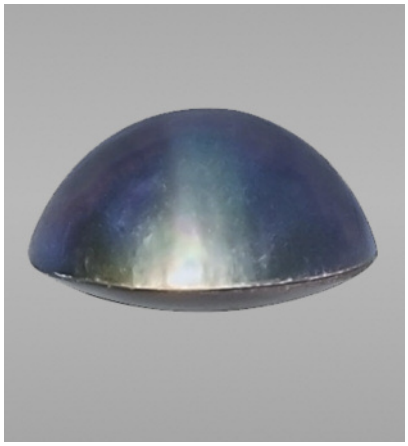

Figure 19. Left: The cross-section revealed the white fluted object with a spiderweb structure bordering the shell base. Right: DiamondView imaging showed a moderate white blue reaction following the spiderweb pattern.

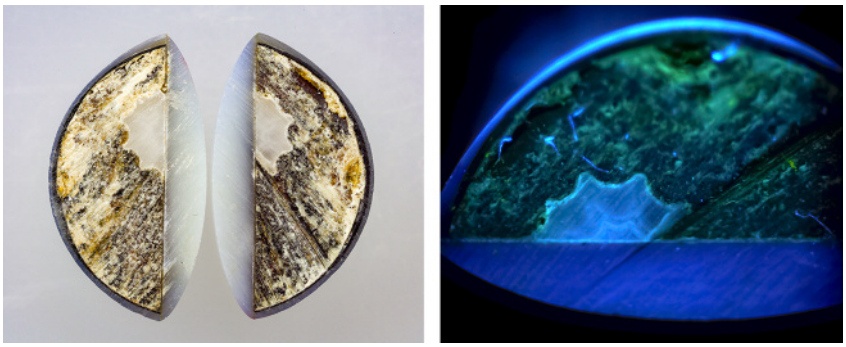

Figure 20. Three unique abalone pearls are shown alongside a typical 12 mm golden South Sea bead-cultured pearl for comparison.

Three Unique Large Natural Pearls from *Haliotis* (Abalone) Species

Natural abalone pearls are produced by many species of the *Haliotis* genus, which are ear-shaped saltwater univalve gastropods. They may form in many different sizes and shapes, though they are commonly encountered in baroque shapes, often taking the form of elongated "horns" and "teeth." The pearls are also notable for their high luster and attractive multicolored appearance, which is usually dominated by blue, green, or yellowish green bodycolors. GIA has reported on many *Haliotis* pearls in previous Lab Notes over the years (Fall 1984, p. 169; Spring 1996, pp. 47–49; Fall 2004, pp. 259–260; Spring 1993, p. 51).

Three large and unique abalone pearls from a client's collection were recently submitted to the New York laboratory (figure 20). Each piece was remarkable in its own right. A button-shaped pearl, measuring approximately 26 × 24 mm with impressive vivid "peacock" blue and green hues, was set in a yellow metal brooch. The second piece, seen in figure 20 on the far right, was a loose abalone pearl weighing 66.83 ct and measuring approximately 42 × 26 × 19 mm with a striking resemblance to a fish's head. The eye, mouth, and gill features were clearly outlined in the specimen, which possessed a smooth surface and subtle array of iridescent greenish yellow colors. The third piece, weighing 113.58 ct and measuring approximately 62 × 29 × 16 mm, was also loose and resembled the head of a snake. It exhibited strong iridescence with mottled patches of various colors

Figure 21. All three specimens from figure 20 showed concentric and void-related internal structures typical of abalone pearls.

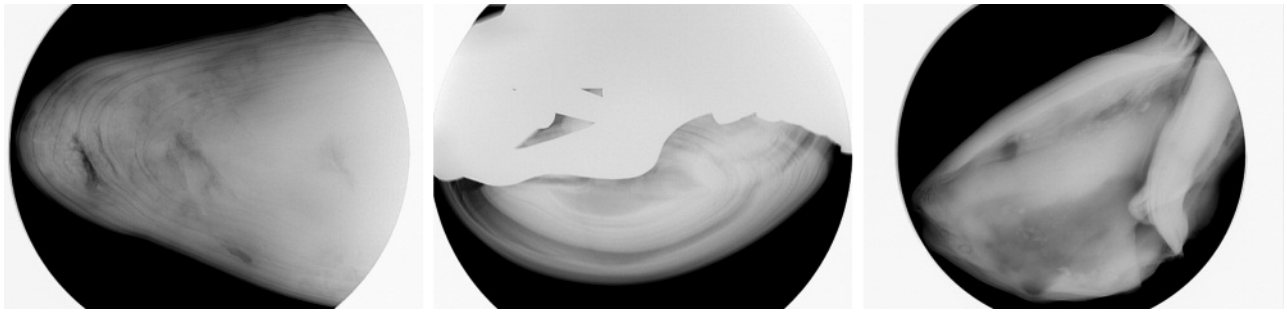

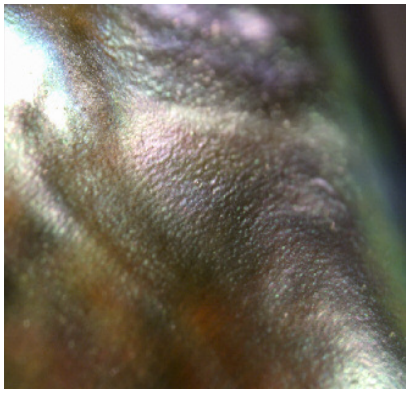

Figure 22. This photomicrograph shows the patches of color and botryoidal-like subsurface structure characteristic of abalone pearls. Field of view 3.9 mm.

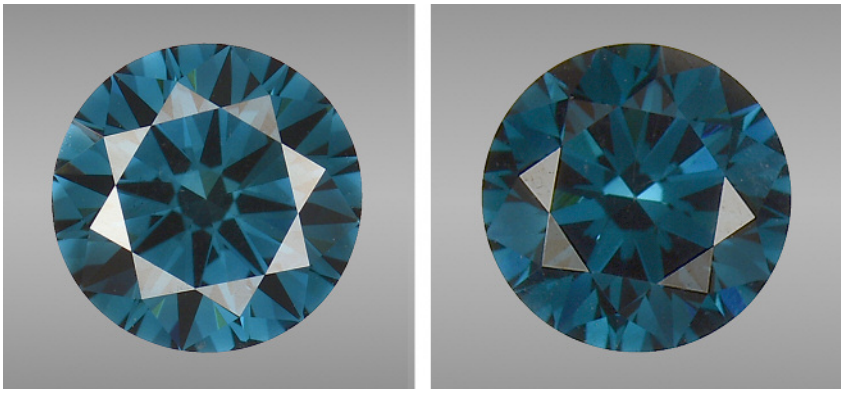

Figure 23. These intensely colored CVD synthetic diamonds, weighing 0.64 ct (left) and 0.43 ct (right), are color graded as Fancy Deep green-blue and Fancy Deep greenish blue, respectively.

similar to the pattern observed on the scaly skin of snakes.

Microradiography revealed characteristic *Haliotis*-related voids with concentric growth structures in all three pearls (figure 21). Two of the pearls also revealed an iodine-rich composition, which GIA has noted is a fairly consistent property of abalone pearls. Such internal structures, along with their distinctive multicolored orient, bubble-like (botryoidal) subsurface structure (figure 22), interesting chemical composition, and chalky greenish yellow fluorescence under long-wave UV are all characteristic of abalone pearls.

The various shapes are determined by where the pearls are formed within the body of the mollusk, and often mirror the form of the gonad (E. Strack, *Pearls*, Ruhle-Diebener-Verlag GmbH & Co. KG, Stuttgart, 2006). Examining all three specimens at the same time allowed us to see a range of colors and shapes possible in abalone pearls. We look forward to encountering more of these unusual pearls.

Joyce Wing Yan Ho and Surjit Dillon Wong

Irradiated Green-Blue CVD SYNTHETIC DIAMONDS

As-grown CVD synthetic diamonds are routinely treated in order to create attractive colors. Irradiated CVD synthetic diamonds without a multi-step treatment process are rarely seen in the lab, though an irradiated Fancy Deep gray-blue CVD synthetic has been reported (Fall 2014 Lab Notes, pp. 240–241). The New York lab recently examined two such examples: a 0.64 ct Fancy Deep green-blue and a 0.43 ct Fancy Deep greenish blue specimen (figure 23).

Dark inclusions, faint color bands, and chips on the girdle were observed in both specimens under the microscope. Tatami-like strain was also seen in both diamonds under cross-polarized light. DiamondView images revealed parallel green linear

Figure 24. DiamondView images reveal linear striations in the pavilions of the 0.64 ct (left) and 0.43 ct (middle) specimens. A face-up image of the 0.43 ct synthetic shows a yellowish green zone of growth interruption (right).

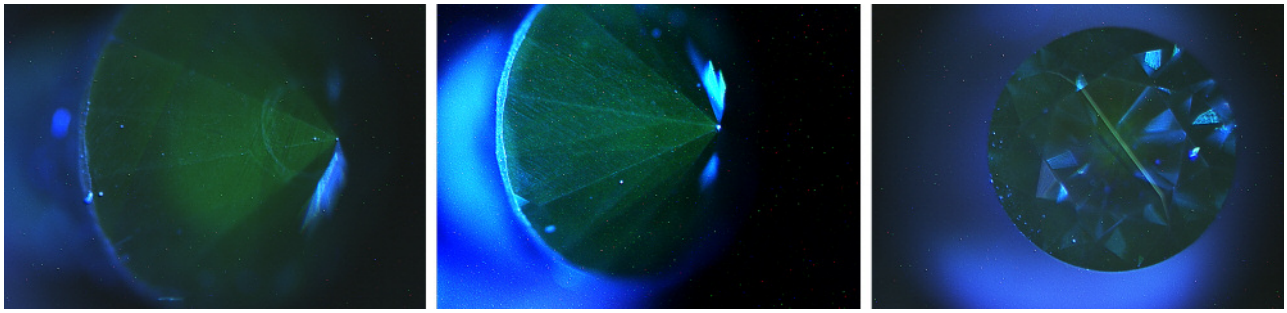

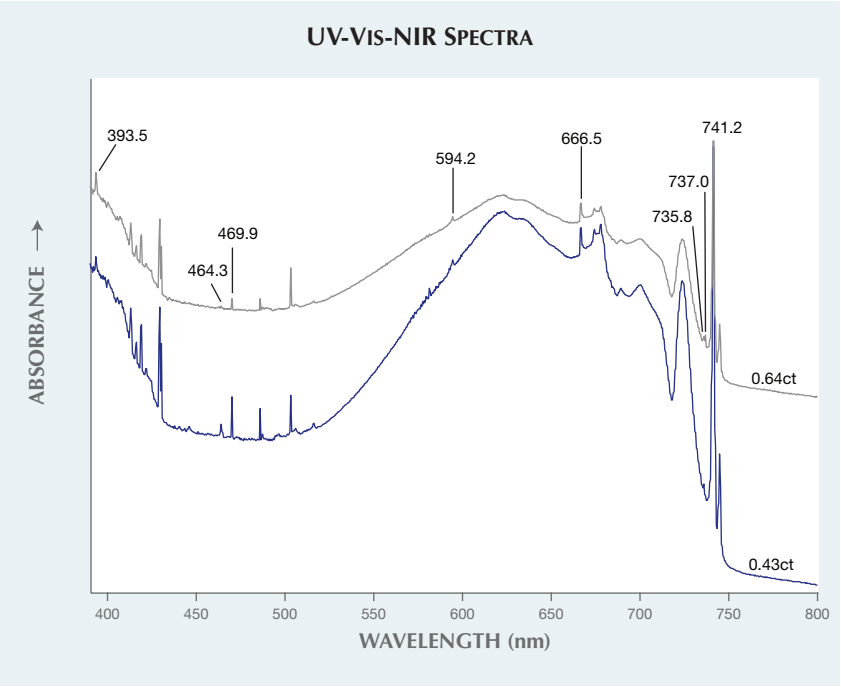

Figure 25. Absorption spectra of the two green-blue CVD synthetics at liquid nitrogen temperature revealed radiation-related peaks. The peaks at 666.5 and 735.8 (both neutral self-interstitial defects) indicate that these samples were annealed at lower temperatures or irradiated without annealing. The Si-V center defect (737.0 nm center) can also be observed at the 736.5–736.9 nm doublet. Many unknown absorption bands (unlabeled in this spectra) are also detected.

striations in the pavilions (figure 24). Face-up DiamondView images also showed yellowish green zones, which were formed by growth interruptions (again, see figure 24). Both stones were pure type IIa diamonds with no other defects in the IR spectra. High-resolution UV-Vis-NIR absorption spectra detected Si-V center defects at the 736.5–736.9 doublet (737 nm center, $(V\text{-}Si\text{-}V)^-$); the spectra also revealed radiation-related peaks at 393.5, 464.3, 469.9, 594.2, 666.5, 735.8, and 741.2 nm (figure 25). The 393.5 band is from the ND1 center, a negatively charged vacancy (V^-). An intrinsic radiation center (TR12) was detected at 469.9 nm. The TR13 center at the 464.3 peak is a local vibrational mode associated with the TR12 center, and the 594.2 band (595 nm center) is a typical radiation-induced center. The 666.5 peak is attributed to a neutral self-interstitial (I^0) defect. The 735.8 band, also caused by the I^0 defect, is related to the 666.5 band. Strong absorption from the GR1 center, which contains neutral vacancies (V^0), was detected at 741.2 nm. All these radiation-related peaks can be destroyed by HPHT treatment, while peaks at 666.5 and 735.8 nm can be annealed out at temperatures ranging from 420° to 540°C (see A.T. Collins, "Spectroscopy of defects and transition metals in diamond," *Diamond and Related Materials*, Vol. 9, Nos. 3–6, 2000, pp. 417–423). The presence of these peaks indicates that these CVD synthetics were either annealed at lower temperatures (<420° to 540°C) or irradiated without annealing.

Although microscopic features such as strain pattern can be helpful in the identification of CVD synthetics, they are not conclusive. DiamondView imaging is very useful for this purpose due to its ability to detect linear striations. As CVD growth techniques continue to improve, we anticipate that intensely colored, high-quality CVD synthetic diamonds will become more prevalent in the trade.

Kyaw Soe Moe, Ulrika D'Haenens-Johansson, and Wuyi Wang

Polished Freeform TOPAZ Imitating Diamond Rough

Topaz is one of many near-colorless diamond simulant materials that may be faceted to bear a closer resemblance to diamond. Although most diamond simulants in the marketplace are faceted, every now and then, one comes across what appears to be a near-colorless octahedron diamond rough (see Lab Notes: Fall 1996, p. 205; Fall 1997, pp. 217–218; Fall 2007, p. 250; Fall 2009, pp. 230–231). A near-colorless 13.70 ct stone (figure 26) was recently submitted to the New York laboratory as a rough diamond from an alluvial source. At first glance, even with a well-trained eye, this stone could easily be misidentified. It bore a striking resemblance to diamond rough, with a "well-formed" octahedral shape and trigon-like formations on the surface

Figure 26. The 13.70 ct topaz under daylight-equivalent light. Note the triangular features on each of the octahedral faces.

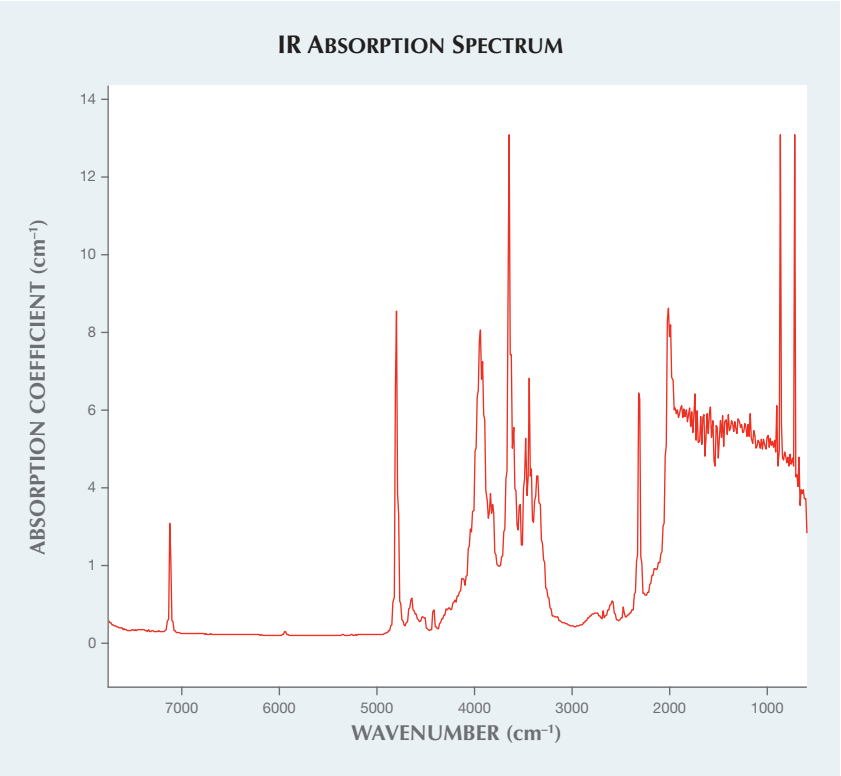

Figure 27. Many absorption peaks related to the hydroxide ion in the crystal structure of topaz are detected in this infrared absorption spectrum, including those at 4802 and 3650 cm^{-1}. These have never been documented in any diamond absorption spectrum.

of each of the faces. To further complicate the identification of this stone, topaz and diamond have the same heft due to overlapping specific gravities: 3.52 (+/-0.10) for diamond, 3.53 (+/-0.04) for topaz. The material was doubly refractive, with a spot RI reading of 1.61, properties consistent with topaz. Final confirmation came from Fourier-transform infrared (FTIR) spectroscopy, which revealed the distinctive topaz absorption spectrum shown in figure 27, with peaks at 4802 and 3650 cm^{-1} (K. Shinoda and N. Aikawa, "IR active orientation of OH bending mode in topaz," *Physics and Chemistry of Minerals*, Vol. 24, No. 8, 1997, pp. 551–554).

Although topaz can be easily shaped and polished into an octahedral shape, the trigon-like figures observed on the surface require an additional fabrication step and are not typically seen in octahedral-shaped simulants. Intentional material processing steps to mask a stone's identity remind gemologists of the caution and care that need to be taken when dealing with gemstone identification—even when the identity of the material initially seems obvious.

Akhil Sehgal and Riccardo Befi

PHOTO CREDITS:
Nathan Renfro—1, 9; Jian Xin (Jae) Liao—2, 26; Robison McMurtry—8, 11, 12, 15; Jonathan Muyal—5, 6, 7, 13; Amy Neurauter—16; Lhapsin Nillapat—17; Areeya Manustrong—18; Sasithorn Engniwat—19 (left); Artitaya Homkrajae—19 (right); Sood Oil (Judy) Chia—20, 23; Surjit Dillon Wong—21; Joyce Wing Yan Ho—22; Kyaw Soe Moe—24.